Available online at www.sciencedirect.com
ScienceDirect
Physics Procedia 3 (2010) 1437–1441
Physics Procedia
www.elsevier.com/locate/procedia

Electronic structure of solid FeO at high pressures by quantum Monte Carlo methods

Jindřich Kolorenč[a*] and Lubos Mitas[a]

[a]Department of Physics and Center for High Performance Simulation, North Carolina State University, Raleigh, North Carolina 27695, USA

We determine equation of state of stoichiometric FeO by employing the diffusion Monte Carlo method. The fermionic nodes of the many-body wave function are fixed by a single Slater determinant of one-particle orbitals extracted from spin-unrestricted Kohn-Sham equations utilizing a hybrid exchange-correlation functional. The calculated ambient pressure properties agree very well with available experimental data. At approximately 65 GPa, the atomic lattice is found to change from the rocksalt B1 to the NiAs-type inverse B8 structure.

Understanding high-pressure behavior of transition metal oxides is of particular importance for condensed matter physics, since amount of electronic correlations changes with compression and it is, therefore, an experimentally tunable quantity. These oxides are among the simplest compounds exhibiting non-trivial effects of correlations, which makes them an ideal medium for investigation of these phenomena. Moreover, iron oxide subject to large pressures is relevant for geophysical applications, since it is an end-member of an important constituent of the Earth's interior, $Fe_{1-x}Mg_xO$.

At ambient conditions, FeO crystallizes in the B1 (NaCl-type) structure. It is paramagnetic at high temperatures and antiferromagnetically ordered below 198 K. This ordering is accompanied by a small rhombohedral distortion—the unit cell is stretched along the [111] body diagonal. Shock-wave studies showed that around 70 GPa the oxide transforms to a different structure [1]. X-ray diffraction performed during the high-temperature static compression revealed that the high-pressure structure is inverse B8 (NiAs-type), iB8 for short [2, 3]. Assessing the correct energy ordering of structural phases of FeO proved to be difficult for the density functional theory (DFT) in the local density and generalized gradient approximations (LDA and GGA). These approaches predict the iB8 phase more stable than B1 at all pressures, clearly contradicting experimental findings [3–5]. It has been demonstrated that inclusion of Coulomb U alleviates this problem [4, 5].

In this paper, we present equation of state of stoichiometric FeO obtained with the fixed-node diffusion Monte Carlo (DMC) method [6], a many-body computational approach that is well suited for strongly correlated systems. Main lines of this calculation were previously reported in Ref. 7. We focus on the two key lattice structures identified in

*On leave from Institute of Physics, Academy of Sciences of the Czech Republic, Na Slovance 2, CZ-18221 Praha 8, Czech Republic; kolorenc@fzu.cz

doi:10.1016/j.phpro.2010.01.203

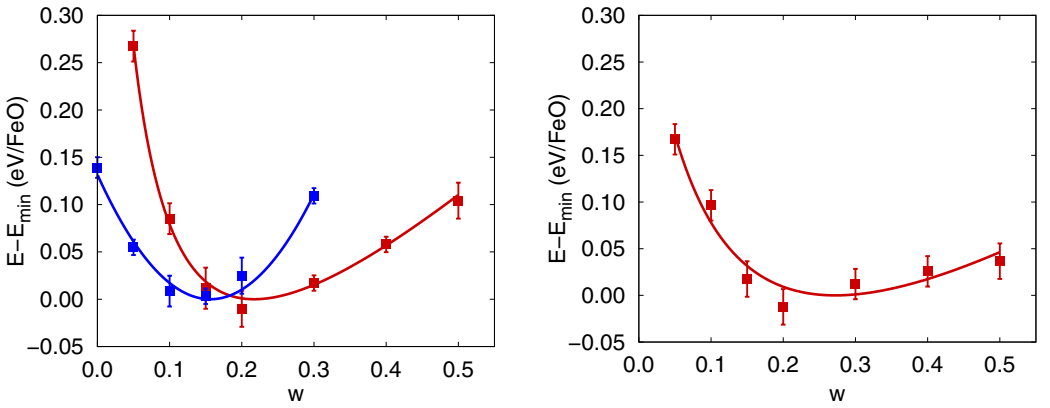

Figure 1. DMC total energy as a function of the exact-exchange weight w calculated in simulation cells containing 8 FeO units. Compressed B1 (red, $V = 17.3$ Å^3/FeO) and iB8 (blue, $V = 17.0$ Å^3/FeO) phases on the left, B1 phase at ambient conditions (red, $V = 20.4$ Å^3/FeO) on the right.

experiments—B1 with the type-II antiferromagnetic (AFM) ordering (space group R$\bar{3}$m) and iB8 also in the AFM state (group P$\bar{6}$m2)—and show that the DMC method provides a consistent picture that closely follows experimental data.

The guiding wave function that determines (fixes) the fermionic nodes in our DMC simulations is of the Slater–Jastrow type, $\Psi_G = \Psi_S \exp[J]$, where

$$\Psi_S(\mathbf{r}_1, \ldots, \mathbf{r}_N) = \det\{\psi_\sigma\} = \det\{\phi^\uparrow_\alpha\} \det\{\phi^\downarrow_\beta\}\,, \tag{1a}$$

$$J(\mathbf{r}_1, \ldots, \mathbf{r}_N) = \sum_{i,j} f(\mathbf{r}_i - \mathbf{r}_j) + \sum_{i,I} g(\mathbf{r}_i - \mathbf{R}_I)\,. \tag{1b}$$

The lower-case indices in Eq. (1b) run over electrons, the upper-case index denotes ions. The Jastrow correlation factor J contains electron–electron and electron–ion terms, f and g, that have the same form as in Ref. 8 and include 17 parameters optimized within the variational Monte Carlo framework. The determinant of spinorbitals ψ_σ becomes a product of determinants of spin-up and spin-down spatial orbitals $\{\phi^\uparrow_\alpha, \phi^\downarrow_\beta\}$ after fixing the electron spins, $N^\uparrow = N^\downarrow = N/2$, while the overall state is a spin-unrestricted antiferromagnet.

The quality of the fixed-node DMC total energy is entirely determined by fermionic nodes of the guiding wave function. The closer these nodes approximate the exact ones, the lower (and therefore more accurate) is the DMC estimate of the ground state energy. The fermionic nodes of a wave function given by Eq. (1) are controlled by the one-particle orbitals $\{\phi^\uparrow_\alpha, \phi^\downarrow_\beta\}$, which we extract from Kohn-Sham equations corresponding to the hybrid exchange-correlation functional PBE0 given as [9]

$$E_{xc}^{PBE0} = wE_x^{HF} + (1-w)E_x^{PBE} + E_c^{PBE}\,. \tag{2}$$

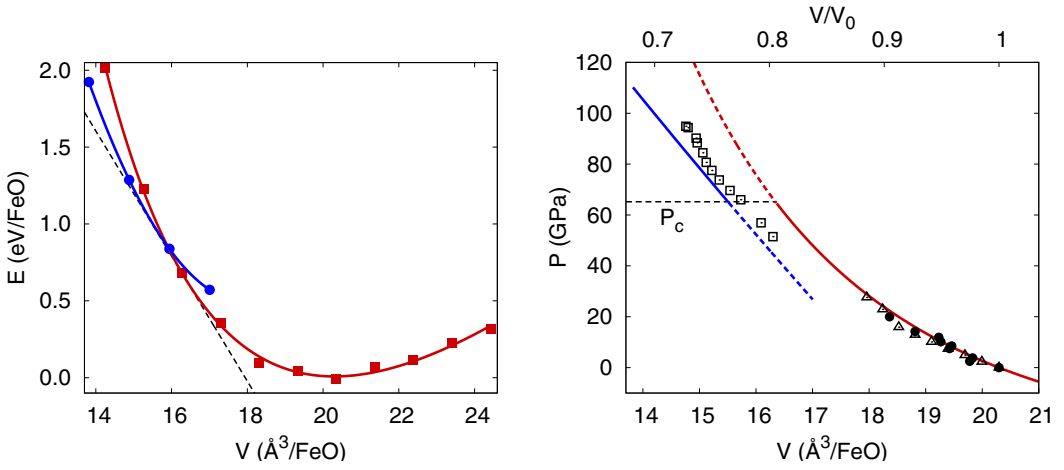

Figure 2. $E(V)$ and $P(V)$ equations of state. Shown are DMC total energies of the B1 (red squares) and the iB8 (blue circles) phases. Statistical error bars are smaller than the symbol sizes. Solid lines are fits with Murnaghan equation of state. Black points represent experiments: circles [15] (B1, $Fe_{0.98}O$), triangles [16] (B1, $Fe_{0.94}O$), squares [2] (iB8, $Fe_{0.98}O$). All B1 data were taken at room temperature, the iB8 data at 900 K. B1 datasets are shown relative to the equilibrium volume to reduce non-stoichiometry effects.

Here E_x^{PBE} and E_c^{PBE} are exchange and correlation parts of the PBE-GGA [10], E_x^{HF} is the exact exchange from Hartree–Fock theory and the weight w is in the range $0 < w < 1$. The functional of Eq. (2) defines a class of one-particle orbitals $\left\{\phi_\alpha^{\uparrow(w)}, \phi_\beta^{\downarrow(w)}\right\}$ than can be used to minimize the DMC fixed-node error by varying the weight w [11]. The DMC total energy as a function of the weight w is plotted in Fig. 1. The optimum is close to 0.25 at ambient conditions and slightly decreases with compression. Since detailed optimization at each volume is computationally expensive, we have fixed the weight w to a reasonable compromise value $w = 0.2$ in our calculation of the equation of state.

The large energy scale associated with core electrons severely limits efficiency of all-electron DMC simulations. Consequently, we replace the atomic cores by norm-conserving pseudopotentials within the so-called localization approximation [12]. We employ small-core pseudopotentials [13, 14] to minimize biases caused by elimination of the core states.

We represent the infinite crystal by a periodically repeated simulation cell containing 8 FeO units, i.e., 176 valence and semi-core electrons. Despite such a large number of electrons, finite-size errors turn out to be significant if not treated properly. One part of these errors is related to incorrect momentum quantization due to confinement of electrons into the simulation cell, the second part comes from the artificial periodicity of the exchange-correlation hole introduced by Ewald sum. To eliminate the first part of the bias, we average over the so-called twisted boundary conditions as proposed in Ref. 17. We have found that in our simulation cells it is sufficient to consider only as few as 8 twists. The second part of the finite-size errors is accounted for by a correction introduced in Ref. 18. This correction is quite effective in the present case, residual errors

Table 1
Equilibrium lattice constant a_0, bulk modulus K_0 and its derivative $K_0' = (\partial K_0/\partial P)_T$ calculated in this work (DMC and PBE0 with $w = 0.2$) compared to selected theories and room-temperature experiments. The experimental a_0 is extrapolated to the stoichiometric FeO, the experimental K_0 and K_0' correspond to $Fe_{0.943}O$ [19] or $Fe_{0.99}O$ [20].

	a_0 (Å)	K_0 (GPa)	K_0'
LDA [21]	4.136	173	4.2
GGA [5]	4.28	180	3.6
PBE0 ($w = 0.2$)	4.328	182	3.7
DMC	4.324(6)	170(10)	5.3(7)
experiment	4.334 [22]	152.3 [19], 175(5) [20]	4.92 [19]

are below statistical uncertainty of our simulations (≈ 0.02 eV/FeO) as demonstrated in Ref. 7.

We impose the cubic symmetry for the low-pressure B1 phase, i.e., the rhombohedral distortion accompanying the antiferromagnetic ordering is neglected. We have checked the impact of this restriction on the DMC total energies at high compression, where the effect is enhanced. Allowing the distortion lowered the total energy only by an amount comparable to the statistical error bars on our data. In the high-pressure iB8 phase, the c/a ratio has been optimized within the DFT utilizing the PBE0 functional with $w = 0.2$.

Results. The DMC energy is plotted as a function of volume in Fig. 2 together with fitted Murnaghan equations of state. Parameters of the least-square fits are compared with other electronic structure methods and with experiments in Tab. 1. The DMC estimates are in very good agreement with experimental values and the Monte Carlo method is consistently accurate for all quantities.

The pressure $P_c = 65 \pm 5$ GPa of the structural transition from the B1 to the iB8 phase has been determined from equality of Gibbs potentials, $G_{B1}(P_c) = G_{iB8}(P_c)$. The error bar is given by statistical uncertainties of the Monte Carlo data. Our result corresponds to low temperatures, where experiments suggest considerably higher transition pressure. Relative stability of the B1 and the iB8 phases could be altered by iron deficiency (non-stoichiometry) and associated lattice defects that are always present in experimental samples. Properties of equation of state around ambient conditions illustrate that effects of non-stoichiometry can be quite sizeable [20]. A reduced stability of the iB8 phase caused by departure from the ideal FeO lattice can be deduced from experiments on closely related materials. For instance, no iB8 is observed in $Fe_{1-x}Mg_xO$ even with as little as 5% of Mg in the sample [23].

In summary, we have used the diffusion Monte Carlo method to study stoichiometric iron oxide at elevated pressures and low temperatures. We have shown that this essentially parameter-free first-principles approach to electronic structure provides an equation of state of FeO that agrees very well with many aspects of available experimental data.

We acknowledge support by NSF EAR-0530110 and DOE DE-FG05-08OR23336 grants. This study was enabled by INCITE and CNMS allocations at ORNL and by allocation at

NCSA. Monte Carlo simulations were done using QWalk code [24], the one-particle orbitals were calculated with Crystal2003 [25]. The gaussian basis used in Crystal2003 was saturated so that the LDA equation of state from Crystal2003 matched the LDA equation of state determined within the linearized augmented plane wave method.

References

[1] R. Jeanloz, T. J. Ahrens, Geophys. J. R. Astr. Soc. 62 (1980) 505–528.
[2] Y. Fei, H. Mao, Science 266 (1994) 1978–1980.
[3] I. I. Mazin, Y. Fei, R. Dawns, R. Cohen, Am. Mineral. 83 (1998) 451–457.
[4] Z. Fang, K. Terakura, H. Sawada, T. Miyazaki, I. Solovyev, Phys. Rev. Lett. 81 (1998) 1027–1030.
[5] Z. Fang, I. V. Solovyev, H. Sawada, K. Terakura, Phys. Rev. B 59 (1999) 762–774.
[6] W. M. C. Foulkes, L. Mitas, R. J. Needs, G. Rajagopal, Rev. Mod. Phys. 73 (2001) 33–83.
[7] J. Kolorenč, L. Mitas, Phys. Rev. Lett. 101 (2008) 185502.
[8] L. K. Wagner, L. Mitas, J. Chem. Phys. 126 (2007) 034105.
[9] J. P. Perdew, M. Ernzerhof, K. Burke, J. Chem. Phys. 105 (1996) 9982–9985.
[10] J. P. Perdew, K. Burke, M. Ernzerhof, Phys. Rev. Lett. 77 (1996) 3865–3868.
[11] L. Wagner, L. Mitas, Chem. Phys. Lett. 370 (2003) 412–417.
[12] L. Mitáš, E. L. Shirley, D. M. Ceperley, J. Chem. Phys. 95 (1991) 3467–3475.
[13] Y. Lee, P. R. C. Kent, M. D. Towler, R. J. Needs, G. Rajagopal, Phys. Rev. B 62 (2000) 13347–13355.
[14] I. Ovcharenko, A. Aspuru-Guzik, W. A. Lester, Jr., J. Chem. Phys. 114 (2001) 7790–7794.
[15] T. Yagi, T. Suzuki, S. Akimoto, J. Geophys. Res. 90 (1985) 8784–8788.
[16] R. L. Clendenen, H. G. Drickamer, J. Chem. Phys. 44 (1966) 4223–4228.
[17] C. Lin, F. H. Zong, D. M. Ceperley, Phys. Rev. E 64 (2001) 016702.
[18] S. Chiesa, D. M. Ceperley, R. M. Martin, M. Holzmann, Phys. Rev. Lett. 97 (2006) 076404.
[19] I. Jackson, S. K. Khanna, A. Revcolevschi, J. Berthon, J. Geophys. Res. 95 (1990) 21671–21685.
[20] J. Zhang, Phys. Rev. Lett. 84 (2000) 507–510.
[21] D. G. Isaak, R. E. Cohen, M. J. Mehl, D. J. Singh, Phys. Rev. B 47 (1993) 7720–7731.
[22] C. A. McCammon, L. Liu, Phys. Chem. Minerals 10 (1984) 106–113.
[23] T. Kondo, E. Ohtani, N. Hirao, T. Yagi, T. Kikegawa, Phys. Earth Planet. Inter. 143-144 (2004) 201–213.
[24] L. K. Wagner, M. Bajdich, L. Mitas, J. Comput. Phys. 228 (2009) 3390–3404.
[25] V. Saunders, R. Dovesi, C. Roetti, R. Orlando, C. M. Zicovich-Wilson, N. M. Harrison, K. Doll, B. Civalleri, I. Bush, P. D'Arco, M. Llunell, CRYSTAL2003 User's Manual, University of Torino, Torino, 2003.